

## CHARACTERIZATION OF VARIOUS ORGANIC WASTE NANOFILLERS OBTAINED FROM OIL PALM ASH

H. P. S. Abdul Khalil,<sup>\*a</sup> Rus Mahayuni A. R.,<sup>a</sup> Irshad-ul-Haq Bhat,<sup>b</sup> Rudi D.,<sup>a,c</sup> M. Z. Almulali,<sup>d</sup> and C. K. Abdullah<sup>a</sup>

The byproducts of palm oil production (nut shells, fibers, and EFB) were combusted to obtain organic waste nanofillers. The prepared nano-filler was characterized by different techniques, viz. XRD for degree of crystallinity, particle size, morphology, and spectroscopic methods. The average diameter found was between 93.39 and 192.20 nm, and the width was between 18.17 and 43.45 nm. The SEM images revealed various morphological arrangements of particles. XRD studies exhibited crystalline nature of both the raw and ground nanofillers. The elemental analysis of nanofillers was carried out by EDX, and FT-IR was used to assign the degree of stretching of various functional groups. In addition to C, N, and O, elemental analysis revealed the presence of Al, Mg, Si, P, K, Ca, Fe, S, Ti, and Mn.

*Keywords:* Oil palm ash; Nanofillers; SEM; XRD; FT-IR

*Contact information:* a: School of Industrial Technology, Universiti Sains Malaysia, Penang, 11800, Malaysia; b: Faculty of Earth Sciences, Universiti Malaysia Kelantan, Campus Jeli, 17600, Kelantan c: School of Life Sciences and Technology, Institute of Technology Bandung, Winaya Mukti 01 Jatinangor Sumedang 45363 West Java Indonesia; d: Building Technology, School of Housing Building and Planning Universiti Sains Malaysia, Penang, 11800, Malaysia; \* Corresponding author: akhalilhps@gmail.com

### INTRODUCTION

The environmental concerns of burning and disposing the residues of combustible substances have grown in recent years (Lee *et al.* 2005). The ash is one of the main concerns, and substantial amounts are obtained by burning of paper, rubbish, and coal (Lee *et al.* 2005). In addition, improper handling of agricultural biowaste also leads to environmental and health problems. Waste disposal from palm oil mills in Malaysia is one of the main environmental challenges for industries after meeting the demand for oil at domestic and global levels (MPOB 2008). Malaysia alone produces millions of tons of oil palm biomass viz. oil palm trunks, oil palm fronds, empty fruit bunches, and therefore, the disposal of such biomass poses a great threat to the ecosystem (Ismail and Shaari 2009). Researchers have utilized the biomass obtained from this source in a sustainable economic way, for the automotive industries, paper technology, composite fabrications, and activated carbon (Abdul Khalil *et al.* 2011). The conversion of biowaste from palm oil to palm oil ash (OPA) is an alternative method to utilize this biowaste in a socio-economic way. Palm oil ash is composed of silicates and aluminates, in addition to different metal oxides and hence can be exploited in various applications viz. as a cement replacement, as a metal adsorbent due to its varied degree of surface area, and further processing. For instance, grinding and ball milling can generate nanoparticles, which can be explored as nanofillers for composite fabrications (Tay and Show 1996; Chu and Hashim 2002; Abdul Khalil *et al.* 2011). Nanotechnological aspects of this biowaste will

allow for a variety of applications either for daily products or for high end advanced products. Researchers have been applying different methods for producing the ash with nano size, using grinding techniques, high end ball milling, sol gel synthesis, and electro-deposition, *etc.* (Cao 2004). These techniques can be used for different materials either on small scale or large scale quantities. The mechanical deformation of these particles leads to formation of crystalline and amorphous material with nanometric size (Koch 2006). Thus, we herein report a study on different OPA ashes obtained at different stages and the conversion of OPA into ground nano-sized ash particles. The raw as well as ground OPA was characterized by using various techniques. The resulting nano-size material obtained can be studied as reinforcement in the fabrication of biocomposites.

## **EXPERIMENTAL**

### **Material**

The oil palm ash (OPA) was obtained from the United Oil Palm Mill, Penang. The precursors for OPA generation were nut shells, fibers, and EFB, which were combusted at 300 °C. Four types of OPA ashes were collected from the particulate collection equipment attached to the stacks of oil palm waste-fired boilers in the palm oil mills.

### **Particle Size**

Measurements of particle size of ground OPA were assessed on a Malvern Zetasizer Nano Series by dynamic light scattering measurements by means of a 532 nm laser. The measurement of the average particle size was automatically repeated three times based on the equipment internal setting.

### **Field Emission Scanning Electron Microscope Studies**

The surface morphology and elemental composition of raw and ground OPA were examined by means of a Carl-Zeiss SMT Leo Supra 50 VP Field Emission Scanning Electron Microscope (FESEM) equipped with an Oxford Instrument Energy Dispersive X-ray (EDX) microanalysis system. Prior to examination, the samples were gold coated with a Fisons Polaron sputter coater.

### **Transmission Electron Microscope Studies**

A Philips-CM12 Transmission Electron Microscope (TEM) was used for the morphology and particle size analysis. Prior to the examination, the ground OPA samples were mixed with water and a drop of the solution was dropped onto a Carbon coated 200 mesh copper grid. The grids were placed on delicate-task-wipers to absorb excess liquid and were left to dry for 10 minutes.

### **X-Ray Diffraction Studies**

The X-ray diffraction (XRD) measurements were carried out on a Philips PW1050 X-pert Diffractometer using CuK $\alpha$  radiation ( $K\alpha = 1.54 \text{ \AA}$ ) at an accelerating voltage of 40 kV and a current of 25 mA. The samples of the raw and ground OPA were scanned in the range from 5 to 90° of  $2\theta$  with a step size of 0.05°. The chemical composition, particle size, and crystallinity were obtained from the diffractograms. From

the broadening of the peak, the average crystallite size was determined with the Debye-Scherrer formula,

$$D = k\lambda / \beta \cos\theta \quad (1)$$

where  $k$  is a constant and is taken as unity,  $\lambda$ -wavelength of the radiation is FWHM (full width half maximum) in radiance of XRD peak obtained at  $2\theta$  and  $D$  is the crystallite size in nm.

### Fourier Transform Infrared Spectroscopy Studies

A Nicolet Avatar 360 Fourier Transform Infrared Spectroscopy (FT-IR) was employed for examining the functional groups on the raw and ground OPA. The powder samples were ground with spectroscopic grade KBr and made into pellets according to the specified sample preparation procedure.

### Preparation of Nanofillers

The raw OPA was ground by using MF 10 basic microfine grinder drive, IKA® WERKE. The grinding involves impact and cutting grinding. The rotor speed was 6500 rotation/min. The filter hole diameter was set to 1.5 mm, 0.5 mm, and 0.25 mm, using MF-sieves of 1.5 mm, 0.5 mm, and 0.25 mm. The samples were sieved by a 20  $\mu\text{m}$  Retsch sieve by means of a stainless steel Retsch sieve shaker, model type 3D. The shaking time was 20 minutes, at amplitude 40. The samples that could pass through the 20  $\mu\text{m}$  sieve were again ground four more times using the 0.25 mm MF-sieves. The samples were labeled as the furnace ash (OPA-R<sub>F</sub>), pit ash (OPA-R<sub>P</sub>), blower ash (OPA-R<sub>B</sub>), and hopper ash (OPA-R<sub>H</sub>). Raw OPA ashes were dried in an oven, ground by a grinder, and were similarly designated as OPA-G<sub>F</sub>, OPA-G<sub>P</sub>, OPA-G<sub>B</sub>, and OPA-G<sub>H</sub>, for furnace ash, pit ash, blower ash, and hopper ash, respectively. All the samples were dried in GOTECH drying oven-GT- 7024 at 70 °C.

## RESULTS AND DISCUSSION

### Characterization of Raw and Ground Oil Palm Ash

#### *Particle size, surface morphology, and elemental analysis*

The average diameter and width of the samples was within the range of 93.39 to 192.20 nm and 18.17 to 43.45 nm, respectively. The range of particles obtained suggests the nano-material nature of OPA. Morphological investigation of the ground palm ash obtained at different stages is given in Fig. 1(a-d). The SEM images revealed medium-sized particles with crushed shape structures. Previous reports on the morphology of oil palm ash have found spongy and porous structures of varied shape (Jaturapitakkul *et al.* 2007). The main components were found to have angular and irregular shapes, although cellular texture has also been reported.

The elemental analysis of OPA is given in Table 1 and 2. The results revealed that the main elements of the raw and ground OPA were Si, C, and O. Other elements present are N, Al, Mg, P, K, Ca, and Fe. It was observed that chlorine was found in OPA-R<sub>B</sub>, ground OPA-G<sub>B</sub>, and OPA-G<sub>H</sub>, at 3.7, 1.8, and 0.07 percent, respectively.

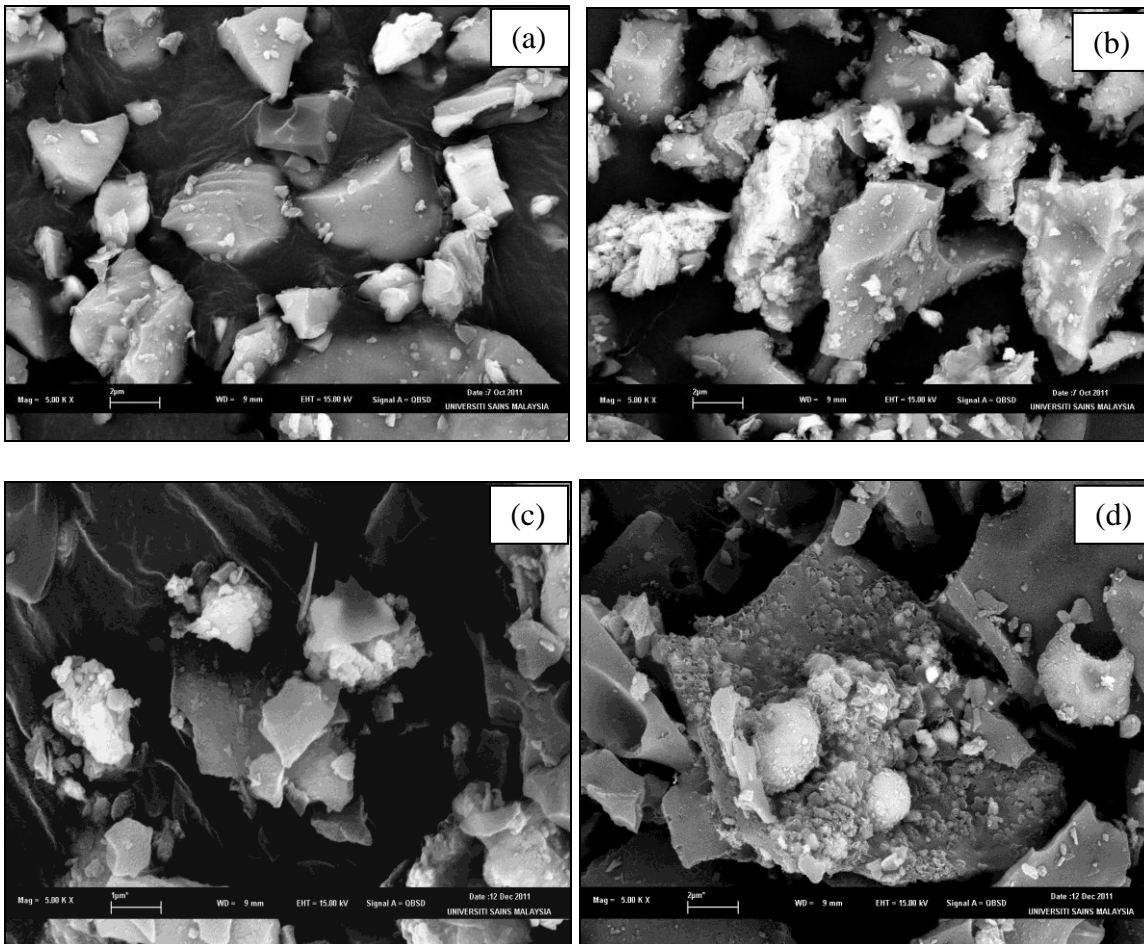


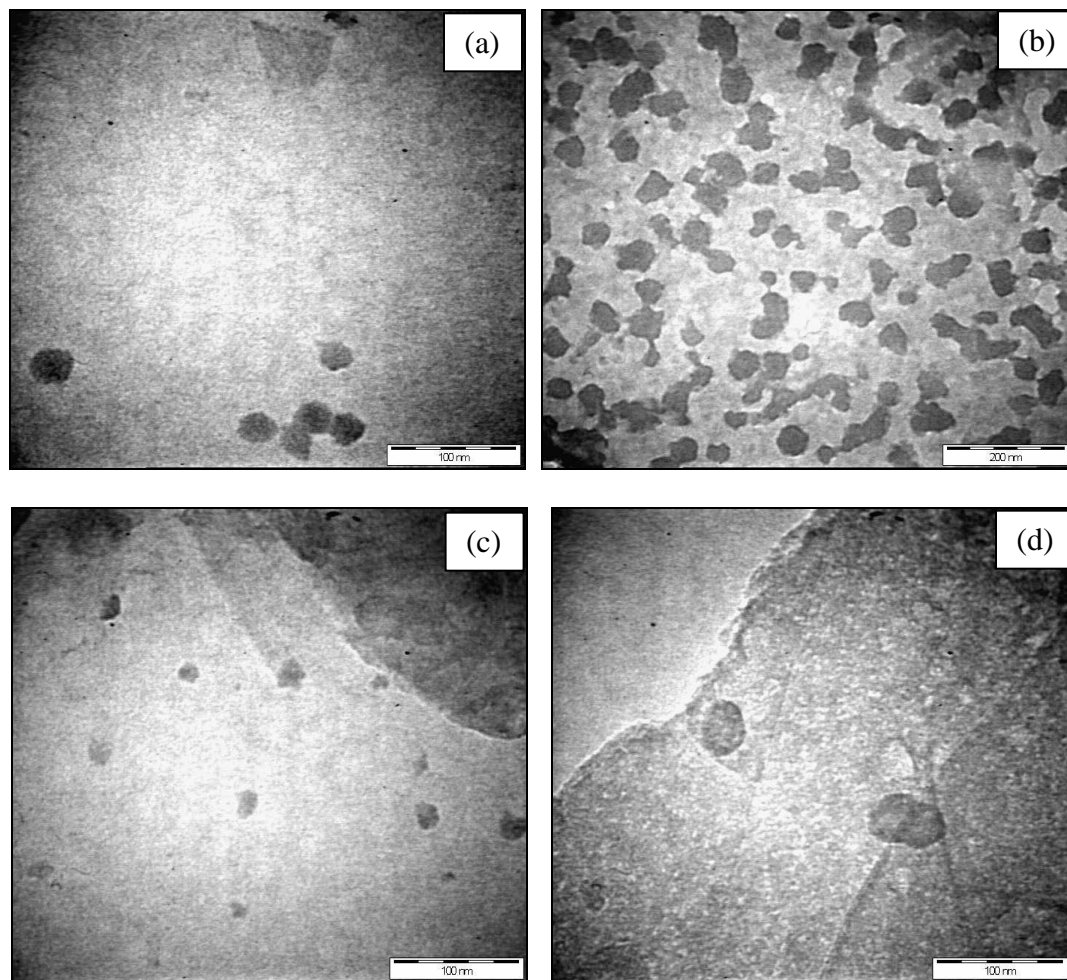
Fig. 1. FESEM (a) (50 x) OPA-G<sub>F</sub>, (b) (50 x) OPA-G<sub>P</sub>, (c) (50 x) OPA-G<sub>B</sub>, (d) (50 x) OPA-G<sub>H</sub>

Table 1. Elemental Composition of the Raw OPA

Element	OPA-R <sub>F</sub>	OPA-R <sub>P</sub>	OPA-R <sub>B</sub>	OPA-R <sub>H</sub>
	Weight %			
C	10.11	9.35	39.55	45.50
N	3.66	3.41	2.18	4.01
O	55.53	46.75	30.81	35.56
Al	0.81	2.85	2.06	0.11
Mg	0.64	1.54	0.25	0.52
Si	24.11	21.50	3.16	12.48
P	0.67	0.28	0.00	0.00
K	2.07	10.67	8.53	1.23
Ca	1.95	2.75	0.99	0.51
Fe	0.45	0.90	8.48	0.08
Cl	0.00	0.00	3.70	0.00
S	0.00	0.00	0.19	0.00
Ti	0.00	0.00	0.10	0.00
Mn	0.00	0.00	0.00	0.00

**Table 2.** Elemental Composition of the Ground OPA

Element	OPA-G <sub>F</sub>	OPA-G <sub>P</sub>	OPA-G <sub>B</sub>	OPA-G <sub>H</sub>
	Weight (%)			
C	8.41	11.30	57.15	48.77
N	5.99	6.90	1.55	6.36
O	44.84	42.97	20.32	32.84
Al	4.37	3.34	0.69	0.10
Mg	1.12	0.59	0.53	1.86
Si	11.31	15.11	8.77	5.31
P	0.81	0.00	0.77	0.86
K	5.41	4.65	5.36	1.98
Ca	2.79	0.75	1.39	1.85
Fe	14.64	14.40	0.36	0.00
Cl	0.00	0.00	1.80	0.07
S	0.00	0.00	1.30	0.00
Ti	0.23	0.00	0.00	0.00
Mn	0.09	0.00	0.00	0.00

**Fig. 2.** TEM micrographs of ground OPA (a) (22k x) OPA-G<sub>F</sub>, (b) (22k x) OPA-G<sub>P</sub>, (c) (22k x) OPA-G<sub>B</sub>, and (d) (22k x) OPA-G<sub>H</sub>

Sulphur was found in raw OPA-R<sub>B</sub> and ground OPA-G<sub>B</sub> with less than 0.19 and 1.3 percent, respectively. Similarly low and very low levels of Ti and Mn were found in OPA-R<sub>B</sub> (0.1%), OPA-G<sub>F</sub> (0.23%), and raw OPA1 (0.09%), respectively. The amount of C and Si was found to be different in OPA-R<sub>F</sub> and OPA-R<sub>P</sub>, with the former having a higher amount of C, and the latter having a higher amount of Si. In the case of OPA-R<sub>B</sub> and OPA-R<sub>H</sub>, the latter contained more C and less Si. Similar results were observed in ground OPA.

The micrographs obtained from TEM studies are given in Fig. 2. The micrographs revealed that ground OPA particles had sizes of less than 50 nm with irregular shapes, indicating their nanometric nature. It was clear by TEM studies that no agglomeration was observed in TEM micrographs. The OPA of this size can be utilized in variety of ways, one being the utilization of OPA as nanofiller in biocomposites (Abdul Khalil *et al.* 2011).

The X-Ray diffraction (XRD) revealed the crystalline nature of both raw and ground OPA. A high intensity peak was observed at 22.6° (2θ) corresponding to the silicates present in both forms of OPA (Abdul Khalil *et al.* 2011; Zainudin *et al.* 2005), while the low intensity peaks can be assigned to other metal oxides present in the OPA (Figs. 3 and 4).

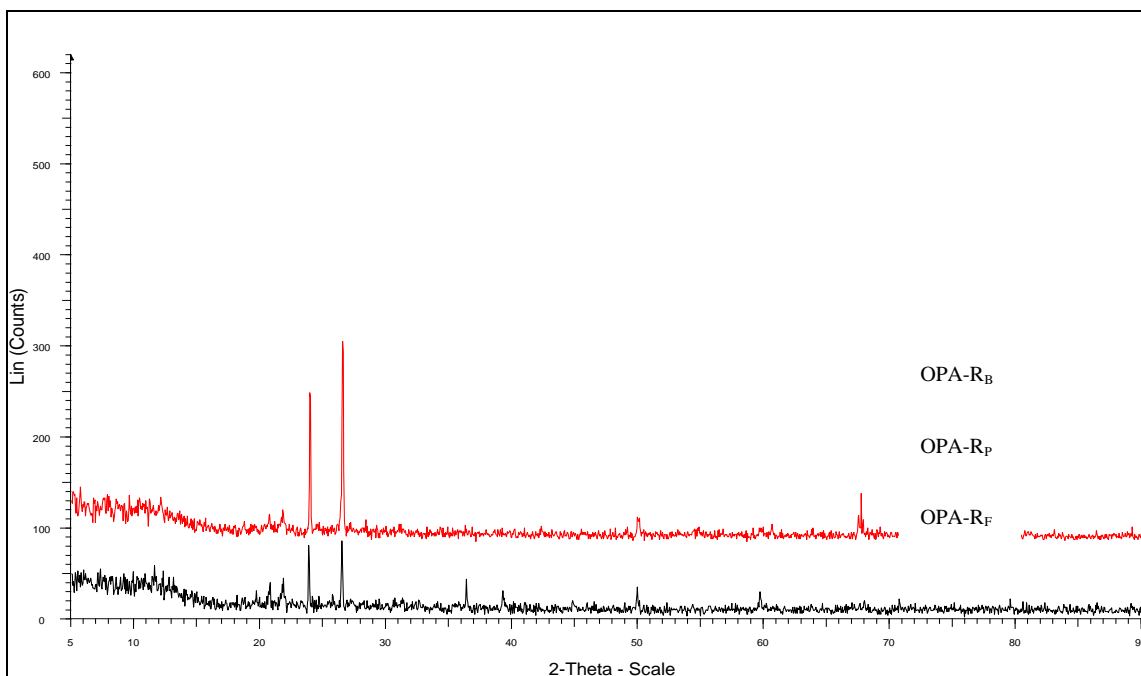


**Fig. 3.** XRD pattern of crystalline raw OPA

The XRD results were well corroborated with the results obtained in EDX studies. It has been found that different elements (C, N, O, Al, Mg, Si, P, K, Ca, and Fe) were present in OPA. XRD results show that all samples contain a low amount of Ti and Mn. The presence of different elements concentrations in OPA is affected by the area of plantation, geographical distribution, quantity of fertilizers used, and agronomy used for the growth of palm oil (Foo and Hameed 2009).

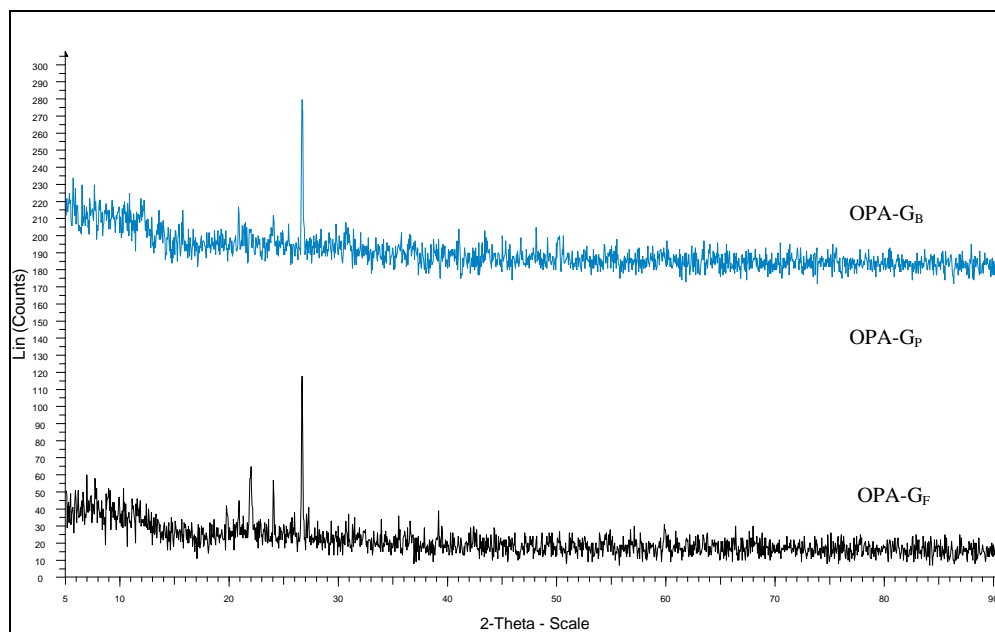


**Fig. 4.** XRD pattern of crystalline ground OPA

A comparative particle size obtained by XRD and a particle size analyzer is given in Table 3. Although different sizes of particles were found by these two different techniques, both techniques revealed that the ground OPA had dimensions of nano-materials with polycrystalline nature.

**Table 3.** Particle Size of Ground OPA Obtained from Particle Size Zetasizer and XRD Methods

Sample	Particle Size ZETASIZER (nm)		XRD
	Diameter	Width	
OPA-G <sub>F</sub>	93.39	19.32	20
OPA-G <sub>P</sub>	144.97	39.93	18
OPA-G <sub>B</sub>	192.20	18.17	26
OPA-G <sub>H</sub>	159.37	43.45	NR

\* NR = not calculated due to amorphous material

## FT-IR CHARACTERIZATION

The FT-IR spectra of raw OPA and ground OPA are given in Figs. 7 and 8. The broad absorption bands observed at 3400 to 3500  $\text{cm}^{-1}$  were ascribed to the stretching vibration of  $-\text{OH}$  groups and silanol hydroxyl groups of silica adhered to the surface of oil palm ash (Ismail and Shaari 2010; Najib 2007)

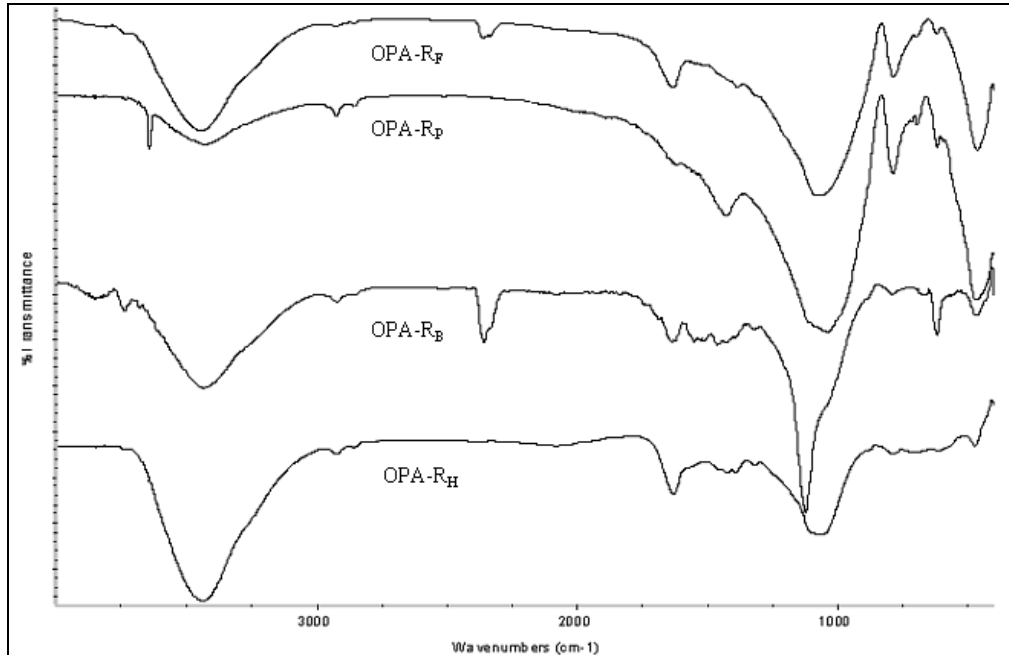


Fig. 5. FT-IR spectra of the raw OPA

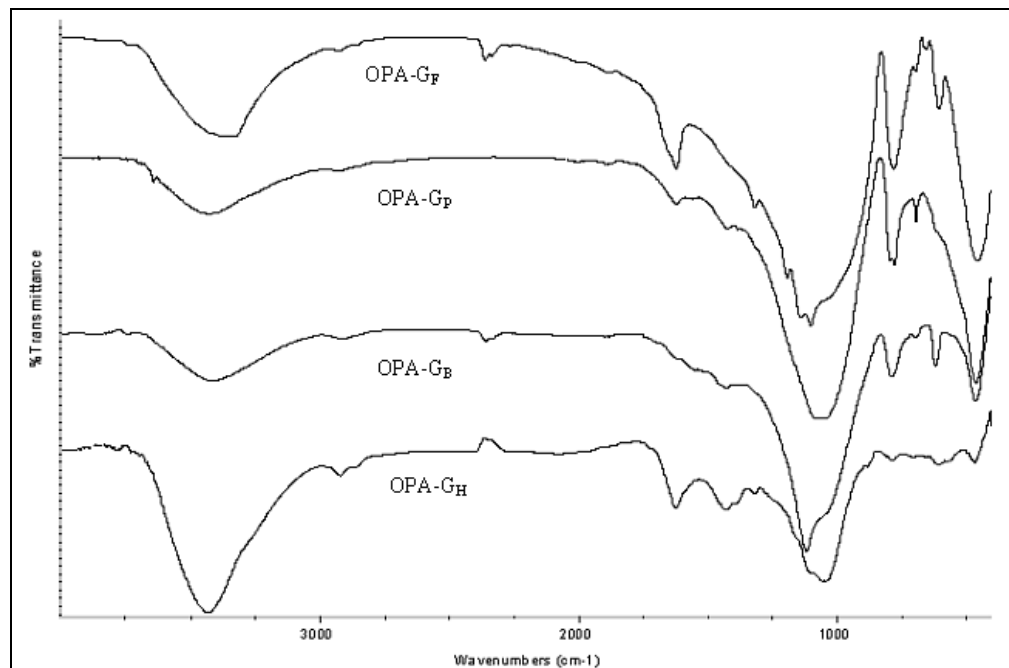


Fig. 6. FT-IR spectra of the ground OPA

The silanols are formed during crushing the ash to fine powdered material. During this process, break-down of the silica structure occurs, leading to the formation of the hydroxyl derivative of silane (Pual *et al.* 2007). The strong and weak bands appearing at  $1050\text{ cm}^{-1}$  and  $800\text{ cm}^{-1}$ , respectively, can be assigned to vibrational frequencies of Al–O or Si–O–Al groups. In addition, weak bands that appeared in this range can be attributed

to deformation which occurred in O-H vibrations bonded to silicon atoms. The band at  $1050\text{ cm}^{-1}$  can be also implied to structural vibration of Si-O bond of  $\text{SiO}_2$  (Hamelmann *et al.* 2005).

## CONCLUSIONS

1. This study analyzed the preparation and characterizations of oil palm ash derived at different particulate stages. The results indicate that various amounts of silica and carbon were present in the raw and ground OPA.
3. The particle size was found to be strongly dependent on the particulate stage. The morphology of particles was found to be like crushed particles.
4. In the FT-IR spectra, in addition to silicon-oxygen vibrations, silanols were also observed.
5. The produced nanomaterials from OPA may be a suitable candidate to be used as nanofiller to reinforced composites.

## ACKNOWLEDGEMENT

The author H. P. S Abdul Khalil highly acknowledges and pays gratitude to the School of Life Sciences and Technology, Institute of Technology Bandung, Winaya Mukti 01 Jatinangor Sumedang 45363 West Java, Indonesia, for providing technical support and facilities during his short visit as a visiting professor.

## REFERENCES CITED

- Abdul Khalil, H. P. S., Fizree, H. M., Jawaidd, M., and Alattas, O. S. (2011). "Preparation and characterization of nanostructured materials from oil palm ash: A bioagricultural waste from oil palm mill," *BioResources* 6(4), 4537-4546.
- Cao, G. (2004). *Nanostructures & Nanomaterials: Synthesis, Properties & Applications*, Imperial College Press, London.
- Chu, K. H., and Hashim, M. A. (2002). "Adsorption and desorption characteristics of zinc on ash particles derived from oil palm waste," *J. Chemical Technol. Biotech.* 77(6), 685-693.
- Foo, K. Y., and Hameed, B. H. (2009). "Value-added utilization of oil palm ash: A superior recycling of the industrial agricultural waste," *J. Hazard. Mater.* 172, 523-531.
- Hamelmann, F., Heinzmann, U., Szekeres, A., Kirov, N., and Nikolova, T. (2005). "Deposition of silicon oxide thin films in TEOS with addition of oxygen to the plasma ambient : IR spectra analysis," *J. Optoelectronics Advanced Materials* 7(1), 389-392.
- Ismail, H., and Shaari, S. M. (2010). "Curing characteristics, tensile properties and morphology of palm ash/halloysite nanotubes/ethylene-propylene-diene monomer (EPDM) hybrid composites," *Polym Testing* 29, 872-878.

- Ismail, H., and Shaari, S. M. (2009). "Curing characteristics, tensile properties and morphology of palm ash/halloysite nanotubes/ethylene-propylene-diene monomer (EPDM) hybrid composites," *Renew Sustain Energy Reviews* 13, 2495-2504.
- Jaturapitakkul, C., Kiattikomol, K., Tangchirapat, W., and Saeting, T. (2007). "Evaluation of the sulfate resistance of concrete containing palm oil fuel ash," *Constr. Build. Mater.* 21, 1399-1405.
- Koch, C. C. (2006). *Nanostructured Materials: Processing, Properties and Applications*, William Andrew Inc., New York, New York, USA.
- Lee, K. T., Bhatia, S., and Mohamed, A. R. (2005). "Preparation and characterization of sorbents prepared from ash (waste material) for sulfur dioxide (SO<sub>2</sub>) removal," *J. Mater. Cycles Waste Manag.* 7, 16-23.
- MPOC- Malaysian Palm Oil Council Available from [http://www.mpoc.org.my/main\\_ind\\_01.asp](http://www.mpoc.org.my/main_ind_01.asp) [cited on 21 December 2008]
- Najib, N. (2007). "Thermoplastic elastomer composites of palm ash filled ethylene vinyl acetate/natural rubber (EVA/NR) blends," M.Sc thesis, Malaysia: Universiti Sains Malaysia.
- Tay, J.-H., and Show, K.-Y. (1996). "Utilization of ashes from oil-palm wastes as a cement replacement material," *Water Sci Technol.* 34(11), 185-192.
- Zainudin, N. F., Lee, K. T., Kamaruddin, A. H., Bhatia, S., and Mohamed A. R. (2005). "Study of adsorbent prepared from oil palm ash (OPA) for flue gas desulfurization," *Sep Purif Technol* 45(1), 50-60.

Article submitted: April 26, 2012; Peer review completed: June 24, 2012; Revised version received: July 17, 2012; Accepted: October 6, 2012; Published: October 17, 2012.